



Cite this: *Nanoscale*, 2015, 7, 11352

## Highly luminescent and cytocompatible cationic Ag<sub>2</sub>S NIR-emitting quantum dots for optical imaging and gene transfection†

Fatma Demir Duman,<sup>a</sup> Ibrahim Hocaoglu,<sup>a</sup> Deniz Gulfem Ozturk,<sup>b</sup> Devrim Gozuacik,<sup>b</sup> Alper Kiraz<sup>a,c</sup> and Havva Yagci Acar<sup>\*a,d,e</sup>

The development of non-toxic theranostic nanoparticles capable of delivering a therapeutic cargo and providing a means for diagnosis is one of the most challenging tasks in nano-biotechnology. Gene therapy is a very important mode of therapy and polyethyleneimine (PEI) is one of the most successful vehicles for gene transfection, yet poses significant toxicity. Optical imaging utilizing quantum dots is one of the newer but fast growing diagnostic modalities, which requires non-toxic, highly luminescent materials, preferentially active in the near infrared region. Ag<sub>2</sub>S NIRQDs fit to this profile perfectly. Here, we demonstrate the aqueous synthesis of cationic Ag<sub>2</sub>S NIRQDs with a mixed coating of 2-mercaptopropionic acid (2MPA) and PEI (branched, 25 kDa), which are highly luminescent in the NIR-I window ( $\lambda_{em} = 810-840$  nm) as new theranostic nanoparticles. Synergistic stabilization of the QD surface via the simultaneous use of a small molecule and a polymeric material provided the highest quantum yield, 150% (with respect to LDS 798 at pH 7.4), reported in the literature for Ag<sub>2</sub>S. These cationic particles show a dramatic improvement in cytocompatibility even without PEGylation, a strong optical signal easily detected by confocal laser microscopy and effective conjugation and transfection of the green fluorescence protein plasmid (pGFP) to HeLa and MCF-7 cell lines (40% efficiency). Overall, these Ag<sub>2</sub>S NIRQDs show great potential as new theranostics.

Received 12th January 2015,

Accepted 23rd May 2015

DOI: 10.1039/c5nr00189g

www.rsc.org/nanoscale

## Introduction

Gene therapy has emerged as a very promising method in the fight against genetic disorders. The major issue in gene therapy is the safe delivery of the gene to the target. Potential gene vectors should condense and protect nucleic acids effectively.<sup>1</sup> So far, two major approaches utilized in nucleic acid delivery are the use of viral and non-viral delivery vectors. Safety hazards of viral vectors remain a big handicap despite

their high transfection efficiency. Non-viral vectors are usually cationic liposomes, dendrimers or polymers.<sup>2-5</sup> One of the best performing synthetic materials is known as polyethyleneimine (PEI). PEI can easily penetrate into cells and disrupt endosomal organelles due to the “proton sponge effect” and release its cargo.<sup>6-8</sup> The transfection efficiency of PEI is molecular weight dependent and increases with increasing molecular weight, yet high molecular weight PEI has significant toxicity as well. So, dosing requires a critical balance of these two factors.<sup>9</sup>

Semiconductor quantum dots (QDs) are the new class of fluorescent probes used for cellular, molecular and *in vivo* imaging applications, due to their stable and size-tunable fluorescence. Narrow emission, a broad absorption window, large molar extinction coefficient, and high chemical stability are also major advantages of QDs over organic fluorophores which make them promising optical imaging agents.<sup>10-12</sup> The majority of the examples in the literature involve QDs with luminescence in the visible region. However, in the visible window, photons are scattered and absorbed by biological constituents such as hemoglobin. Near-infrared (NIR) fluorescence is most favorable for biological applications since it provides a higher penetration depth into the tissues than

<sup>a</sup>Koc University, Graduate School of Materials Science and Engineering, Rumelifeneri Yolu, Sariyer, 34450 Istanbul, Turkey. E-mail: fyagci@ku.edu.tr; Fax: +902123381559; Tel: +902123381742

<sup>b</sup>Sabanci University, Faculty of Engineering and Natural Sciences, Molecular Biology, Genetics Biological Sciences and Bioengineering Programs, Orhanli-Tuzla, 34956 Istanbul, Turkey

<sup>c</sup>Koc University, Department of Physics, Rumelifeneri Yolu, Sariyer, 34450 Istanbul, Turkey

<sup>d</sup>Koc University, Department of Chemistry, Rumelifeneri Yolu, Sariyer, 34450 Istanbul, Turkey

<sup>e</sup>KUYTAM, Koc University Surface Science and Technology Center, Rumelifeneri Yolu, Sariyer, 34450 Istanbul, Turkey

† Electronic supplementary information (ESI) available. See DOI: 10.1039/c5nr00189g

visible light, lower background fluorescence, lower signal loss, and thus a greater signal-to-background ratio.<sup>13,14</sup> The absorption by biological constituents is minimal between 700 and 1300 nm and QDs emitting in this region are by far more advantageous for biological applications, especially for *in vivo* imaging.<sup>15–18</sup> Such potential accelerated the development of NIR-emitting quantum dots such as PbSe,<sup>19</sup> PbS,<sup>20</sup> and CdHgTe.<sup>21</sup> However, the intrinsic toxicity of Pb, Cd, or Hg is a significant limitation.<sup>22</sup> Therefore, biocompatible NIRQDs would be best suited as optical imaging agents and Ag<sub>2</sub>S NIRQDs seem to satisfy this requirement.<sup>23–30</sup> Ag<sub>2</sub>S show a low release of Ag<sup>+</sup> ions rendering it highly cytocompatible.<sup>24,31</sup> Wang *et al.* produced hydrophobic Ag<sub>2</sub>S NIRQDs emitting at 1058 nm from (C<sub>2</sub>H<sub>5</sub>)<sub>2</sub>NCS<sub>2</sub>Ag<sup>32</sup> and then the PEGylated ones *via* ligand exchange with DHLA and conjugation with PEG. These Ag<sub>2</sub>S NIRQDs emitting at 1200 nm showed enhanced spatial resolution in the *in vivo* imaging of angiogenesis<sup>33</sup> and allowed the tracking of mesenchymal stem cells *in vivo*.<sup>34</sup> In the last four years a large amount of effort has been directed to the aqueous synthesis of Ag<sub>2</sub>S NIRQDs. Tian *et al.* synthesized water-soluble Ag<sub>2</sub>S quantum dots coated with 3-mercaptopropionic acid and demonstrated their use as an optical probe in the *in vivo* studies using mice.<sup>23</sup> Cui and Su *et al.* synthesized Ag<sub>2</sub>S NIRQDs using RNase A as a template in aqueous medium *via* the biomimetic route.<sup>24</sup> Pang *et al.* prepared emission-tunable Ag<sub>2</sub>S quantum dots in a two-step procedure.<sup>25</sup> Yan *et al.* reported bovine serum albumin (BSA)-stabilized NIR emitting Ag<sub>2</sub>S NIRQDs and their conjugation with the endothelial growth factor (VEGF) antibody for targeted cancer imaging.<sup>26</sup> Wang *et al.* studied the long-term *in vivo* effect and biodistribution of PEGylated-Ag<sub>2</sub>S NIRQDs. The prepared QDs accumulated in the RES (reticuloendothelial system), especially in the liver and spleen and cleared from the body by fecal excretion.<sup>27</sup> Hocaoglu and Acar reported one of the first examples of a simple aqueous synthesis of highly luminescent and cytocompatible Ag<sub>2</sub>S quantum dots which were stabilized with 2-mercaptopropionic acid.<sup>35</sup> These Ag<sub>2</sub>S NIRQDs have the highest QY reported in the literature so far with 39%, upon aging. Effective imaging properties of Ag<sub>2</sub>S NIRQDs were demonstrated in mammalian cells for the first time in the literature and enhanced cytocompatibility was shown even at extremely high doses (up to 200 μg mL<sup>-1</sup>).

One of the most important factors for obtaining good quality QDs is surface passivation. The packing density of the coating material on the crystal surface and the binding strength are also important. Uncoordinated sides on the crystal surface may act as defects and cause non-radiative coupling events, causing relatively low luminescence intensity. As optical probes, QDs with strong luminescence are highly desirable as they would provide a better signal-to-noise ratio and may allow the usage of lower doses. Previously, we have shown that when a mixture of a polymeric material and a small thiolated ligand is used as a coating for CdS, both the ability to tune the crystal size and the quantum yield of CdS QDs are improved dramatically.<sup>36</sup> Also, we have demonstrated that 2MPA is a much more advantageous coating when

compared to the widely used 3-MPA, in terms of the stability and luminescence intensity of the resulting QDs due to the interaction of carboxylate groups with the crystal surface in addition to thiol binding, which was shown by *ab initio* calculations and supported by lifetime measurements.<sup>37</sup> Therefore, Ag<sub>2</sub>S NIRQDs were synthesized with a mixed coating of bPEI (25 kDa) and 2MPA in order to obtain highly luminescent, stable and cationic nanoparticles.

Here, we report the development of the first NIR emitting cationic Ag<sub>2</sub>S NIRQD-based theranostic material designed as a gene delivery vector and as an optical imaging agent. In order to achieve high transfection efficiency, low cytotoxicity, strong luminescence and cytocompatibility, mixtures of branched PEI (25 kDa) and 2MPA were utilized as the direct coating of Ag<sub>2</sub>S nanocrystals in an aqueous synthesis procedure. In almost all the related literature wherein cationic QDs were developed, PEI was either covalently attached to the Cd-chalcogenides which were initially coated with materials comprising carboxylic acid and in general were further functionalized with PEG to reduce the toxicity,<sup>11</sup> or electrostatically bound to the anionic QD surface<sup>38,39</sup> or deposited on the QD surface *via* ligand exchange of the initial fatty acid or similar coatings.<sup>40</sup> Yet, these approaches usually produce large size agglomerates and/or reduce the quantum yield. Besides, in addition to its advantages, PEGylation also brings about issues such as reduced functional sites for oligonucleotide binding, decreased surface charge and interference with endosomal escape of the particles.<sup>11</sup> There is one report focusing on the synthesis of CdS/ZnS QDs directly coated with PEI (10 kDa) in water but the luminescence is weak and the molecular weight of the PEI is low for effective transfection.<sup>41</sup> There are two studies that we are familiar with which incorporate NIRQDs with PEI: (1) CdPbS coated with a silica shell was electrostatically bound to PEI, but at PEI/QD ratios where agglomeration was prevented, the luminescence intensity dropped dramatically.<sup>42</sup> These particles were not utilized for transfection of any plasmid or drug and no data on cytotoxicity were available for the comparison. (2) CdTe based quantoplexes produced by mixing mercaptoacetic acid coated CdTe, DNA and PEI and their biodistribution was studied *in vivo*.<sup>43</sup> These quantoplexes were about 200 nm in size and had very low quantum yield (15% of Alexa Fluor 750 which has a quantum yield of 12%). In addition, there was a significant amount of uncomplexed PEI in the formulation, which is an important drawback. Therefore, achieving a good quantum yield and a low cytotoxicity added to a good transfection efficiency, especially with non-toxic NIRQDs, is extremely advantageous and we achieved this with the approach described herein.

We have designed these cationic NIRQDs with a cytocompatible NIR emitting QD core, which is Ag<sub>2</sub>S, kept the crystal size small in order to obtain emission in the NIR-I window, which is suitable for fluorescence imaging *in vitro* using a confocal microscope, used the golden standard of synthetic transfection agents, which is the 25 kDa branched PEI, but mixed it with a stable and effective 2MPA to enhance the luminescence efficiency and balance the toxicity coming from the cationic

**Table 1** Effect of PEI/2MPA ratios on the properties of Ag<sub>2</sub>S NIRQDs

Rxn code	PEI <sup>a</sup> (%)	2MPA <sup>a</sup> (%)	Rxn pH	$\lambda_{\text{abs}}^b$ (nm)	Size <sup>c</sup> (nm)	Band gap <i>E</i> (eV)	$\lambda_{\text{em}}^{\text{(max)}}$ (nm)	FWHM (nm)	Dh <sup>d</sup> (nm)	Zeta pot. (mV)
1	100	0	10	906	2.94	1.37	—	—	4.0	51
2	90	10	10	674	2.23	1.48	838	175	2.9	34
3	80	20	10	761	2.48	1.63	819	173	3.5	28
4	60	40	10	777	2.52	1.60	817	168	3.8	36
5	0	100	7.5	806	2.61	1.54	837	128	7.10	-62

<sup>a</sup> Mol%. <sup>b</sup> Absorbance onset measured from the absorbance spectrum (Fig. S6). <sup>c</sup> Diameter of Ag<sub>2</sub>S crystals calculated using the Brus equation.

<sup>d</sup> Hydrodynamic diameter measured by DLS at pH 7.4 and reported as the number average. All reactions were quenched in 5 min.

coating without PEGylation. Also, this strategy allowed us to synthesize these particles directly in aqueous solutions, which eliminated ligand exchange steps. The influence of reaction variables such as coating type, PEI/2MPA ratio, pH and reaction time on the optical properties of the QDs was studied systematically. Aq. Ag<sub>2</sub>S with the highest reported quantum yield was obtained under optimized conditions of synthesis. These are also the first cationic Ag<sub>2</sub>S NIRQDs in the literature. The cytocompatibility of these cationic Ag<sub>2</sub>S QDs was evaluated using the HeLa cell line. The suitability of particles for imaging was demonstrated in the HeLa and MCF-7 cell lines using confocal laser microscopy. The potential of these particles as gene vectors was tested in *in vitro* transfection experiments. The transfection efficiency of PEI-2MPA coated Ag<sub>2</sub>S NIRQDs was determined in HeLa and MCF-7 cells using the green fluorescence protein plasmid (pGFP), and results were compared with a standard transfection agent (25 kDa PEI) in its standard procedure in a standard protocol. This is the first example of gene transfection and optical imaging performed with Ag<sub>2</sub>S NIRQDs *in vitro*.

## Materials and methods

### Materials

All reagents were of analytical grade or of the highest purity. Silver nitrate (AgNO<sub>3</sub>) was purchased from Sigma-Aldrich. Sodium sulfide (Na<sub>2</sub>S) was purchased from Alfa-Aesar. Branched polyethyleneimine (PEI) (*M*<sub>w</sub> 25 kDa) was purchased from Aldrich (Germany). Linear PEI (25 kDa) was purchased from PolySciences, Inc. (USA). Sodium hydroxide (NaOH), 2-mercaptopropionic acid (2MPA), ethanol and acetic acid (CH<sub>3</sub>COOH) were purchased from Merck (USA). The LDS 798 near-IR laser dye was purchased from Exciton, Inc. (USA). Only Milli-Q water (18.2 MOhm) was used when necessary. DMEM medium (with 4500 mg per L glucose, 4.0 mM L-glutamine, and 110 mg per L sodium pyruvate), trypsin-EDTA, penicillin-streptomycin and fetal bovine serum were purchased from HyClone, USA. Thiazolyl blue tetrazolium bromide (MTT) *Bio-Chemica* was purchased from AppliChem, Germany. Paraformaldehyde solution 4% in PBS and UltraCruz™ 96-well plates were purchased from Santa Cruz Biotechnology, Inc., USA.

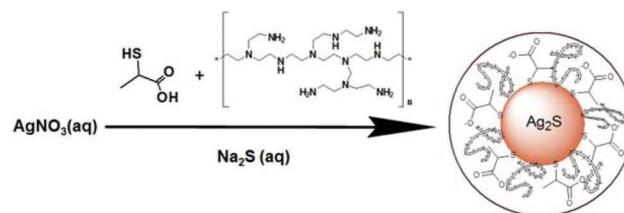
Glass bottom dishes were purchased from MadTek, USA. Dimethyl sulfoxide Hybri-Max™ and phosphate buffered saline (pH 7.4) were purchased from Sigma, USA.

### Preparation of PEI and 2MPA coated Ag<sub>2</sub>S nanoparticles

All reactions were performed under an inert atmosphere. Typically, 42.5 mg of AgNO<sub>3</sub> (0.25 mmol) and 4.9 mg of Na<sub>2</sub>S (0.0625 mmol) were dissolved in 75 ml and 25 mL of deoxygenated water respectively in separate round bottom flasks. PEI and 2MPA in the desired ratios, as listed in Table 1, were added to the AgNO<sub>3</sub> solution, respectively. The total coating/Ag mole ratio was kept constant at 5. For 2MPA, moles of thiol groups, and for PEI, moles of amine groups were considered. As an example, a mixed coating containing 20% 2MPA had 1 equivalent of thiol (0.25 mmol) and 4 equivalents of amine (1 mmol) with respect to Ag. The pH of the final solution was adjusted using NaOH and CH<sub>3</sub>COOH solutions (2.5 M). Na<sub>2</sub>S solution was added to this reaction mixture under vigorous mechanical stirring at 5000 rpm and at room temperature (25 °C). During the reaction, samples were taken at different time points to follow the particle growth. Prepared quantum dot solutions were washed with deionized water using Amicon-Ultra centrifugal filters (30 000 Da cutoff) and stored in the dark at 4 °C (Scheme 1).

## Characterization methods

Absorbance spectra of the prepared Ag<sub>2</sub>S quantum dots were recorded using a Shimadzu 3101 PC UV-Vis-NIR spectrometer in the 300–1100 nm range. Crystal sizes of Ag<sub>2</sub>S nanoparticles

**Scheme 1** Aqueous synthesis of PEI and 2MPA coated Ag<sub>2</sub>S NIRQDs.

were calculated from absorption spectra of the particles using the absorption edge in the Brus equation (eqn (1)):

$$\Delta E = \frac{\hbar^2 \pi^2}{8R^2} \left[ \frac{1}{m_e} + \frac{1}{m_h} \right] - 1.8 \frac{e^2}{\epsilon_{\text{Ag}_2\text{S}} 4\pi\epsilon_0 R} \quad (1)$$

where  $R$  is the radius of the nanocrystal,  $m_e$  (0.286  $m_0$ ) and  $m_h$  (1.096) are the respective effective electron and hole masses for the inorganic core, and  $\epsilon_{\text{Ag}_2\text{S}}$  (5.95) is the dielectric constant and  $\Delta E$  is the band gap energy difference between the bulk semiconductor and the nanocrystal.

A homemade setup was used in the photoluminescence measurements.  $\text{Ag}_2\text{S}$  NIRQDs were excited with a frequency doubled output of a DPSS laser (532 nm). After the luminescence was filtered by a 590 nm long pass filter, it was collected with a 1/8 Newport Cornerstone 130 monochromator having 600 L per mm grating and operating in the 400–1000 nm range. The wavelength selected signals were detected by a femtowatt sensitive Si detector (Thorlabs PDF10A,  $1.4 \times 10^{-15}$  W Hz $^{-1/2}$ ).

For Quantum Yield (QY) calculations, QD samples in water and a NIR dye in methanol were prepared at five different concentrations having absorbance values at the excitation wavelength at or below 0.15. These five concentrations were adjusted in such a way that absorbance values of the dye samples and QD samples were close to each other. The LDS 798 NIR dye (quantum yield reported as 14% in MeOH by the producer) was used as the reference. Photoluminescence of these solutions was recorded at an excitation wavelength of 532 nm, and the integrated areas under the curves were plotted against the absorbance (Fig. S1 and S2†). QY was calculated from the ratio of the slope of these plots, using the refractive index of water and MeOH based on eqn (2), as reported in the literature.<sup>36,44,45</sup>

$$\Phi_{\text{QD}} = \left( \frac{\text{Grad}_{\text{QD}}}{\text{Grad}_{\text{REF}}} \right) \left( \frac{\eta_{\text{water}}^2}{\eta_{\text{MeOH}}^2} \right) \times 100 \quad (2)$$

The XRD pattern of the quantum dots was recorded between  $2\theta$  angles of  $10^\circ$  and  $90^\circ$  using a Bruker D2 Phaser Benchtop XRD system with Cu K $\alpha$  radiation ( $\lambda = 1.5406$  Å). About one gram of the dried sample was placed in between gelatine films. Air bubbles were removed and the sample was placed on a sample holder. TEM analysis of nanoparticles was performed using a JEOL JEM-ARM200CFEG UHR-transmission electron microscope (JEOL, Japan). The hydrodynamic size and zeta potential of the aqueous nanoparticles were measured with a Malvern Zetasizer Nano-ZS. A Thermo Scientific K-Alpha XPS with Al K-alpha monochromatic radiation (1486.3 eV) was used for XPS analysis of QDs. Dried samples were placed on an adhesive aluminum tape. 400  $\mu\text{m}$  X-ray spot size and 50.0 eV pass energy corresponding to a resolution of roughly 0.5 eV were used. The base pressure and the experimental pressure were below  $3 \times 10^{-9}$  mbar and about  $1 \times 10^{-7}$  mbar, respectively. The C 1s peak at 285.0 eV was assigned as the reference signal for the evaluations.

The  $\text{Ag}^+$  concentration of QD solutions was determined using a Spectro Genesis FEE Inductively Coupled Plasma Optical Emission Spectrometer (ICP OES). QDs were exposed to acids (Suprapur nitric acid 65% and Suprapur sulphuric acid 96%) for digestion and diluted to certain volumes. The  $\text{Ag}^+$  ion concentrations in solutions were calculated using a standard curve of the known  $\text{Ag}^+$  ion concentrations.

### Cell lines and cell culture

MCF-7 human breast carcinoma and HeLa cell lines were cultured in DMEM (Sigma, 05671) supplemented with 10% (v/v) fetal bovine serum (FBS; Biochrom KG, S0115) and antibiotics (penicillin/streptomycin; Biological Industries, 03-031-1B) in a 5%  $\text{CO}_2$ -humidified incubator at 37 °C.

### Gene delivery tests

$\text{Ag}_2\text{S}$ -PEI-2MPA mediated transfections were conducted by mixing various concentrations of QDs (according to the measured concentrations of  $\text{Ag}^+$  ions by ICP OES) (1  $\mu\text{g ml}^{-1}$ , 1.5  $\mu\text{g ml}^{-1}$ , 2  $\mu\text{g ml}^{-1}$  and 2.5  $\mu\text{g ml}^{-1}$ ) with 4  $\mu\text{g}$  pMax-GFP vector DNA (Lonza) in 50  $\mu\text{l}$  serum-free DMEM. Mixtures were allowed to incubate for 10 min and were added to cells seeded in 12-well plates (MCF-7: 100 000 cells per well, HeLa: 75 000 cells per well). At six hours post-transfection, cells were washed with PBS and then fresh medium was added. Control transfections were conducted similarly, using the linear 25 kDa polyethyleneimine (PEI) (1  $\mu\text{g ml}^{-1}$ ) as one of the standard transfection agents.

The transfection efficiency was checked 48 h post-transfection. Prior to the analysis, cell nuclei were stained with the Hoechst dye (Invitrogen, 33342) to better assess the ratio of GFP positive cells to the total cell population. Hoechst was added to the cells at a final concentration of 1  $\mu\text{g ml}^{-1}$ . After 20 minutes of incubation, cells were washed with PBS to remove excess amount of the dye. Cells were fixed in 3.7% paraformaldehyde for 20 min, washed with PBS, mounted in 50% glycerol in PBS and inspected under 20 $\times$  or 40 $\times$  magnification using a BX60 fluorescence microscope (Olympus). At least 150 cells per condition were analyzed and results were expressed as a percentage of GFP positive cells *versus* the total number of cells (Hoechst dye positive nuclei). All measurements were repeated in at least 3 independent experiments.

### Cytotoxicity assay

To study the cytotoxicity of the prepared QDs on the HeLa cell line, thiazolyl blue tetrazolium bromide (3-(4,5-dimethylthiazol-2-yl)-2,5-diphenyltetrazolium bromide, MTT) was utilized. Cells were cultured in 96-well plates with complete medium at 37 °C and 5%  $\text{CO}_2$  for 24 h. On the second day, the medium was renewed and QDs were added to the culture medium at different concentrations and incubated for another 24 h. On the third day, cells were washed with PBS. The MTT reaction solution was added to the cells and incubated for 4 h. Purple formazan was dissolved with DMSO : ethanol (1 : 1) by gentle shaking for 15 min. The absorbance of formazan was measured by reading the absorbance at a wavelength of

600 nm with a reference at 630 nm on a microplate reader (BioTek ELx800 Absorbance Microplate Reader). QD absorbance in complete medium was measured as well and was subtracted from the MTT solution to correct the result. Experiments were repeated four times. Statistical analysis was performed with GraphPad Prism software (Graphpad Software, Inc., USA). Columns were compared as pairs by using the one way ANOVA test with Tukey's multiple comparison test or by using a two tailed Student's *t*-test. All data were represented as mean  $\pm$  SD (standard deviation). The confidence level was accepted as 95% (significant at  $p < 0.05$ ).

### Cell imaging

Imaging of HeLa and MCF-7 cells was performed using two different confocal laser scanning microscopes in order to visualize NIR emission of QDs and GFP signals. For QD localization analysis, 50 000 HeLa cells were cultured in glass bottom dishes and incubated for 18 h. Following incubation, the culture medium was replenished and cells were incubated with QD solution which has  $2.5 \mu\text{g mL}^{-1}$  of  $\text{Ag}^+$  ions for 6 h. Cells were washed with PBS (pH 7.2) and fixed with 4% paraformaldehyde for 15 min. Finally, the washing step was repeated and cells were kept in PBS to protect the cells from drying. To detect the intracellular uptake and localization of  $\text{Ag}_2\text{S}$  NIRQDs, a home-made sample scanning confocal microscope system equipped with a Si avalanche photodetector and a  $60\times$  (NA: 1.49) oil immersion objective was used. The excitation laser beam at 532 nm was transmitted through neutral density filters and reflected by a broadband dichroic mirror (Chroma 10/90 beamsplitter). A long pass glass filter RG665 was placed before the detectors to collect the QD emission.

Confocal laser microscopy studies were performed to visualize the green fluorescence in transfected cells by GFP/ $\text{Ag}_2\text{S}$  NIRQDs. Initially, 150 000 MCF-7 or HeLa cells were cultured in 12-well plates with cover slides. After an overnight incubation, transfection with a QD solution (at a concentration of  $2.5 \mu\text{g mL}^{-1}$  of  $\text{Ag}^+$ ) conjugated to the pMax-GFP plasmid was performed. Cells were washed with PBS after 6 hours of incubation. At 48 hours after transfection, cells were fixed in 3.7% paraformaldehyde for 20 min, washed with PBS and mounted in 50% glycerol in PBS. Cells were imaged using a Nikon Eclipse Te2000-U confocal microscope to detect the GFP signal after transfection.

## Results and discussion

### PEI coated NIR-emitting $\text{Ag}_2\text{S}$ quantum dots

Direct aqueous synthesis was utilized in the synthesis of cationic NIR-emitting  $\text{Ag}_2\text{S}$  NIRQDs as a greener and a facile synthesis method. Cationic  $\text{Ag}_2\text{S}$  NIRQDs were synthesized directly in water from  $\text{AgNO}_3$  and  $\text{Na}_2\text{S}$  under an inert atmosphere at room temperature with branched PEI (25 kDa) as a coating. The factors that usually affect the particle size and quality such as the reaction duration and the Ag/S and PEI/Ag ratios were studied to investigate the ability to tune size and

therefore the emission wavelength of QDs, and to find out the conditions which would produce the best luminescing particles within the 700–900 nm range. The pH of the reaction solution was around 9–10 due to the presence of PEI. Results indicated that PEI can stabilize QDs in the aq. medium; however, these variables did not allow efficient size tuning and the luminescence of the particles were poor (Fig. S3 and 4†). In polymer coated particles, due to the lack of dense packing on the particle surface, a significant amount of defects may exist resulting in non-radiative coupling events and hence low luminescence.

### PEI/2MPA coated NIR-emitting $\text{Ag}_2\text{S}$ quantum dots

In order to improve the luminescence quality of  $\text{Ag}_2\text{S}$  NIRQDs and achieve size tunability, mixed coating formulations composed of PEI and 2MPA were used.  $\text{Ag}_2\text{S}$  NIRQDs with only 2MPA coatings were also prepared for comparison of the properties. All particles were synthesized under identical conditions (Table 1). Usually, the reaction time allowed for the crystal growth may act as a factor in tuning the particle size. However, initial experiments done with 100% PEI and 60/40 PEI/2MPA have shown that the particle size or the luminescence peak maximum of the resulting QDs does not change after 5 min (Fig. S5†) following the addition of  $\text{Na}_2\text{S}$ . Therefore, all comparative reactions were quenched in liq. nitrogen at 5 min after sulfide addition.

In the QD synthesis, the pH of the reaction mixture was adjusted to 10 before the addition of  $\text{Na}_2\text{S}$ , except for in the case of 100 mol% 2MPA which was performed at pH 7.5, since the Ag-2MPA complex precipitates at higher pH values. The pH of the PEI solution is usually around 10, but after the addition of 2MPA to the reaction mixture, a significant drop in pH was observed. As an example, pH drops to 7.5–7.8 with 20 mol% 2MPA, and to 3.0–3.5 in the case of 40 mol% 2MPA.  $\text{p}K_a$  of PEI is in the range of 8.2–9.5.<sup>46–48</sup> Protonation of the amines is problematic since they will be originating from the binding of PEI to the QD surface. Thus, pH was readjusted to 10 before the addition of the sulfur source to the reaction mixture.

In comparable reactions in which the Ag/S ratio and the coating/Ag ratio were set at 4 and 5, respectively, only the PEI/2MPA ratio was changed to study the influence of coating composition on particle properties. All reactions with up to 40 mol% 2MPA formed a stable colloidal suspension of QDs with a dramatically improved luminescence intensity over those with 100 mol% PEI coating (Fig. 1). Besides, these QDs also outperformed the luminescence intensity of 100 mol% 2MPA coated  $\text{Ag}_2\text{S}$  NIRQDs which were the best luminescing  $\text{Ag}_2\text{S}$  NIRQDs reported in the literature to date.<sup>35</sup> Amongst the PEI/2MPA coated  $\text{Ag}_2\text{S}$  NIRQDs, the best luminescence intensity was obtained with 20 and 40 mol% 2MPA in the coating mixture (Fig. 1). A non-luminescent bulk material was obtained when 60 mol% 2MPA was used. Therefore, a higher 2MPA content in the mixture was not attempted. Addition of 2MPA as a co-stabilizer also reduced the particle (inorganic crystal) size (Table 1). Actually, all QDs prepared with the mixed coating

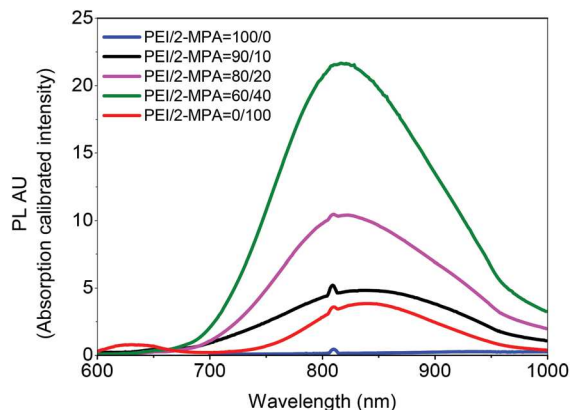


**Fig. 1** Photoluminescence spectra of Ag<sub>2</sub>S NIRQDs prepared with different PEI/2MPA ratios (Ag : S = 4, room temperature, reaction pH: 10, 5 min reaction).

formulations are also smaller than 100 mol% 2MPA coated QDs with better luminescence, indicating a synergy. This is in agreement with the results obtained from poly(acrylic acid)/mercaptoacetic acid coated CdS QDs.<sup>36,49</sup> In the case of polymeric coatings, the lack of dense surface passivation causes poor control of crystal growth and poor surface quality, resulting in large crystals with surface defects possibly originating from nonradiative couplings reducing the quantum yield and the luminescence intensity. Addition of a small thiolated ligand which binds strongly and densely to the surface left uncapped by the polymeric coating both limits crystal growth more effectively and reduces surface defects. As a result, mixed coatings produce smaller particles with better luminescence intensity. Increasing the 2MPA amount decreased the crystal size slightly, causing a slight blue shift in the emission peak (Fig. 1, Table 1). Overall, all Ag<sub>2</sub>S NIRQDs with mixed coatings emit between 817 and 838 nm, which is within the so-called diagnostic window, with a full-width at half-maximum (FWHM) of around 170 nm and better luminescence than 2MPA or PEI coated particles.

Ag<sub>2</sub>S-PEI/2MPA QDs were designed as potential theranostic nanoparticles with cationic surfaces. The zeta potential of the Ag<sub>2</sub>S-PEI is 51 mV and it drops down to -30 mV in the case of Ag<sub>2</sub>S-2MPA (Table 1). Although 2MPA decreases the cationic coating content, QDs with mixed coatings are still cationic enough (*ca.* 30 mV) for possible use as oligonucleotide condensing vectors.

### Influence of the pH on particle properties

Protonation of PEI with the addition of 2MPA is an important issue. Between the pH values of 5.5 and 11 (before the addition of a sulfur source) no significant change in the particle size or the position of emission maximum was observed for Ag<sub>2</sub>S-PEI/2MPA NIRQDs with 20 and 40 mol% 2MPA in the coating composition (Fig. 2 and S7†).

After all, pH had a strong influence on the luminescence intensity. The best luminescence was obtained at pH 10 with 60/40 PEI/2MPA composition and pH 9 for 80/20 PEI/2MPA. In addition, emission peaks with 60/40 PEI/2MPA of Ag<sub>2</sub>S NIRQDs have two emission maxima and have poor colloidal stability at pH values below 9. However, Ag<sub>2</sub>S NIRQDs with 80/20 PEI/2MPA are stable and have strong emission at all pH values. With a motivation to understand the behavior of these QDs in different pH media such as physiological media like blood (~pH 7.4) or in endosome (~pH 5.5), the luminescence of Ag<sub>2</sub>S NIRQDs with 80/20 PEI/2MPA was evaluated at pH 5.5, 7.4 and 9 after being synthesized at pH 9 and washed. As seen in Fig. 3 and S8† and Table 2, the luminescence peak position or absorption onset did not change much with the changes in pH within this range, which indicates that the PEI/2MPA coating provided strong protection to the Ag<sub>2</sub>S core.

As expected, the zeta potential increased substantially with decreasing pH upon protonation of the PEI. This caused a dramatic increase in the quantum yield. There may be two factors responsible for such behavior: (1) a possible disaggregation of particles upon charge repulsion; (2) elimination of free electrons which may act as a hole trap. A major jump in the QY and zeta potential was observed when the pH dropped from 9 to 7.4 where secondary amines were protonated as well. QY

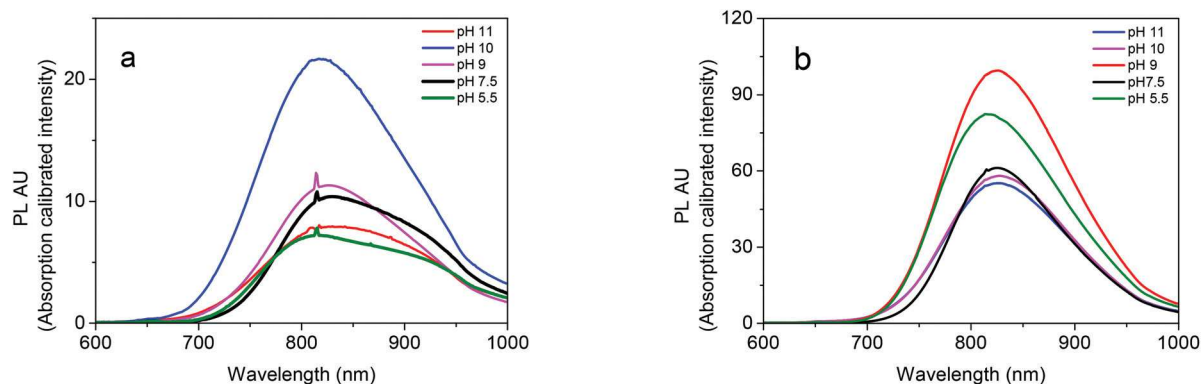


**Fig. 2** Photoluminescence spectra of Ag<sub>2</sub>S NIRQDs prepared with (a) 60/40 PEI/2MPA (Rxn 4) and (b) 80/20 PEI/2MPA (Rxn 3) coating formulation. Spectra were taken after particles were washed and the solution pH was adjusted to 7.4 to prevent differences in intensity based on pH.

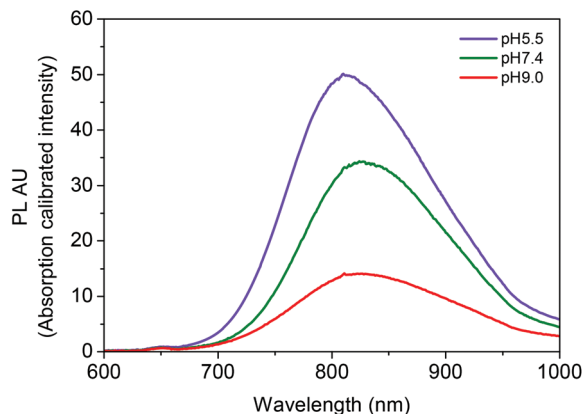


**Fig. 3** Photoluminescence spectra of aqueous  $\text{Ag}_2\text{S}$  NIRQDs at different pH values. NIRQDs were prepared with the 80/20 PEI/2MPA coating formulation, washed and the pH was adjusted ( $\text{Ag}:\text{S} = 4$ ,  $\text{Ag}:\text{PEI} = 1:4$ ,  $\text{Ag}:\text{2MPA} = 1:1$ ,  $T = \text{RT}$ , reaction pH = 9, reaction time = 5 min).

was doubled, reaching a value of 150% with respect to the LDS 798 near-IR dye (quantum yield reported as 14% by the producer). Further acidification to pH 5.5 caused an additional 10% increase in the QY (166%). These QYs are the highest among  $\text{Ag}_2\text{S}$  NIRQDs reported in the literature to the best of our knowledge.

#### Long term stability of $\text{Ag}_2\text{S}$ -PEI/2MPA QDs

Long term colloidal and luminescence stabilities of QDs are crucial for their practical applications. Aqueous QD suspensions were stored in a refrigerator and were analyzed at extended time periods to detect any change in their size, stability or QY (Table 3). All particles stayed well dispersed in water and had no precipitation even after 1 year. During this time period, while the inorganic core size of  $\text{Ag}_2\text{S}$  NIRQDs which was measured with the Brus equation and the emission maximum stayed the same, the QY decreased to 38% in 1 year (Fig. S9†). However, this value is still as high as the highest recorded QY reported so far for  $\text{Ag}_2\text{S}$  NIRQDs.<sup>35</sup>

#### Particle characterization

PEI/2MPA coated  $\text{Ag}_2\text{S}$  NIRQDs are crystalline materials having the size distribution between 2 and 4 nm as depicted by the TEM images (Fig. 4a and b). Broad size distribution is also

possibly originating from broad FWHM of the emission peaks. Crystal structures of the nanoparticles were observed well in the focused images (Fig. 4c and d). The interplanar distance measured from the focused images is 0.221 nm and fits well to the reported values for the 031 plane of monoclinic  $\text{Ag}_2\text{S}$ .<sup>50,51</sup>

XRD analysis did not provide well resolved peaks due to the presence of a polymer (Fig. S10†). However, XPS analysis indicates the formation of  $\text{Ag}_2\text{S}$  (Fig. 5). Ag 3d core level peaks at the binding energies (BE) of 367.41 (3d5/2) and 373.45 (3d3/2) eV fit well to the  $\text{Ag}^+$  of  $\text{Ag}_2\text{S}$ . There are two different S based on the doublets fitted to the S 2p signal: S 2p3/2 at BE of 160.82 eV and 162.05 eV fits to the S-Ag and S of 2MPA, respectively.<sup>35</sup> The N 1s region can be fitted to three peaks at 398.25, 398.75 and 400.56 eV corresponding to tertiary, secondary and primary N of PEI. Based on the literature values reported for primary amines of free PEI (399.84 eV), this shift to higher BE indicates surface binding of primary N and electron donation to QDs.<sup>52</sup>

#### Cytocompatibility of quantum dots

The most stable and most strongly luminescing  $\text{Ag}_2\text{S}$  NIRQDs (80/20 PEI/2MPA) was subjected to *in vitro* cytotoxicity studies. For comparison,  $\text{Ag}_2\text{S}$ -PEI and  $\text{Ag}_2\text{S}$ -2MPA NIRQDs were also subjected to the same tests. Viability of HeLa cells after 24 h incubation with QDs at 1–25  $\mu\text{g Ag}^+$  per mL concentrations, which corresponds to 4.6–115  $\mu\text{g QDs}$  per mL, was determined with the widely used MTT assay (Fig. 7). As seen in Fig. 6, 100% 2MPA coated  $\text{Ag}_2\text{S}$  NIRQDs are not toxic within this dose range as expected based on previously published data.<sup>35</sup> On the other hand, PEI (branched, 25 kDa) is known to be toxic.

To understand its possible contribution to NIRQD toxicity, some amount of PEI coming from the formulation was applied to the HeLa cells as well. As an example, in 4.6  $\mu\text{g}$  nanoparticles per mL, there is 1  $\mu\text{g}$  per mL  $\text{Ag}^+$  (measured by ICP-OES) and 2.8  $\mu\text{g}$  per mL PEI. So, for the 4.6–115  $\mu\text{g QDs}$  per mL dose range, the 2.8–70  $\mu\text{g}$  per mL PEI dose range was tested (Fig. 8). The drop in the cell viability at all doses with respect to the control is statistically significant ( $p < 0.05$ ), but the differences between each concentration of PEI are insignificant. Overall, PEI was highly toxic even at the lowest dose of 2.8  $\mu\text{g mL}^{-1}$  (less than 50% viability). However, binding PEI to the  $\text{Ag}_2\text{S}$  surface improved the cytocompatibility dramatically with respect to free PEI.  $\text{Ag}_2\text{S}$  NIRQDs with 100 mol% PEI or 80/20 PEI/2MPA coatings showed no statistically significant

**Table 2** Influence of pH on the properties of  $\text{Ag}_2\text{S}$ -PEI/2MPA QDs

pH	$\lambda_{\text{abs(cutoff)}}^a$ (nm)	Size <sup>b</sup> (nm)	Band gap (eV)	$\lambda_{\text{em (max)}}$ (nm)	FWHM (nm)	Dh <sup>c</sup> (nm)	Zeta pot. (mV)	QY <sup>d</sup> (%)
5.5	783	2.54	1.59	812	151	9.4	63	166
7.4	783	2.54	1.59	828	150	8.9	60	150
9.0	783	2.54	1.59	825	170	8.0	32	77

<sup>a</sup> Absorbance onset. <sup>b</sup> Crystal diameter calculated using the Brus equation. <sup>c</sup> Hydrodynamic diameter measured by DLS and reported as the number average. <sup>d</sup> Quantum yield calculated with respect to the LDS 798 near-IR dye ( $\text{Ag}:\text{S} = 4$ ,  $\text{Ag}:\text{PEI} = 1:4$ ,  $\text{Ag}:\text{2MPA} = 1:1$ , Temp. = RT, reaction pH = 9, reaction time = 5 min).

**Table 3** Time dependent changes in particle properties<sup>a</sup>

Time	$\lambda_{\text{abs(cutoff)}}^b$ (nm)	Size <sup>c</sup> (nm)	$\lambda_{\text{em(max)}}^c$ (nm)	FWHM (nm)	QY <sup>d</sup> (%)
1 <sup>st</sup> day	783	2.54	828	150	150
1 <sup>st</sup> month	783	2.54	828	150	111
3 <sup>rd</sup> month	783	2.54	828	150	93
9 <sup>th</sup> month	783	2.54	828	150	42
1 year	783	2.54	828	150	38

<sup>a</sup> Ag<sub>2</sub>S NIRQDs synthesized with 80/20 PEI/2MPA coating formulation at pH 9.0 were used. The sample pH was adjusted to 7.4 before measurements. <sup>b</sup> Absorbance onset. <sup>c</sup> Crystal diameter calculated using the Brus equation. <sup>d</sup> Quantum yield calculated with respect to the LDS 798 near-IR dye.

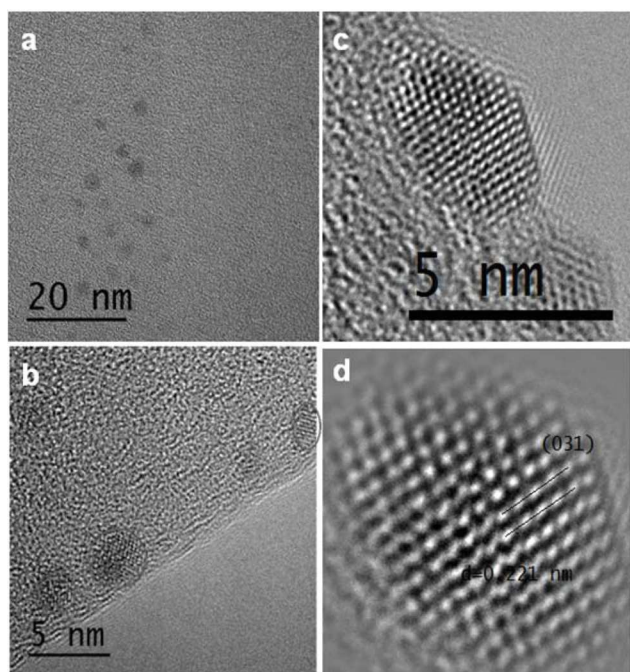


**Fig. 4** TEM images of Ag<sub>2</sub>S NIRQDs (80/20 PEI/2MPA; synthesized at pH 9.0) at different magnifications (a and b); diffraction of the Ag<sub>2</sub>S crystal lattice (c); *d*-spacing determined using a focused image (d).

drop in the cell viability up to 2.5  $\mu\text{g Ag}^+$  per mL, but at 5  $\mu\text{g Ag}^+$  per mL the viability dropped to  $64 \pm 12\%$ . Using a mixed coating at a given Ag<sup>+</sup> concentration meant a lower amount of PEI for the given dose, but the improvement over the pure PEI is much more dramatic than what this 20% less PEI may cause. One possible reason may be the occupation of some amine groups with crystal surface binding. Considering the high cytocompatibility of 2MPA coated Ag<sub>2</sub>S, it is safe to say that toxicity originates from the PEI component. Looking at the similarities between PEI and PEI/2MPA coated particles in cell viability (Fig. 6), it may be reasonable to say that 2MPA did not impact viability much. 2MPA is the smaller size com-

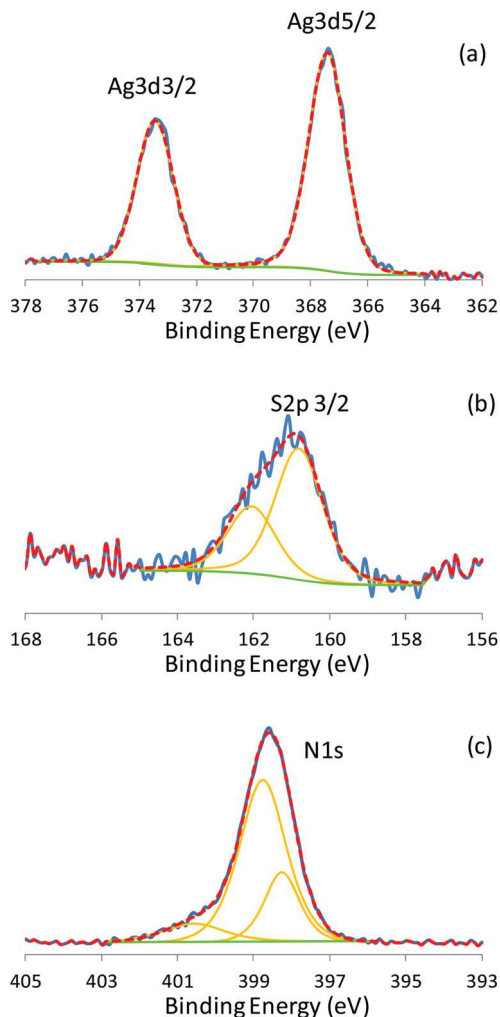


**Fig. 5** (a) Ag 3d, (b) S 2p and (c) N 1s XPS spectra of Ag<sub>2</sub>S–PEI/2MPA (80/20) QDs.

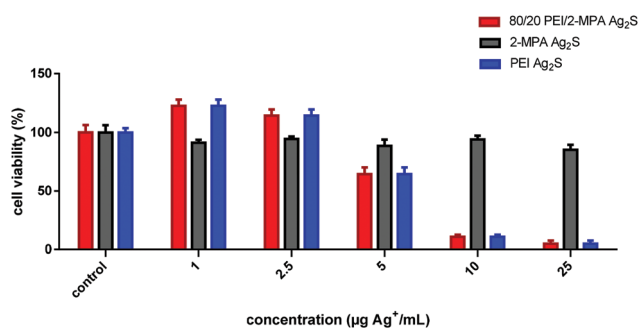


**Fig. 6** Percent viability of HeLa cells exposed to Ag<sub>2</sub>S NIRQDs with PEI, 2MPA and 80/20 PEI/2MPA mixed coatings determined by the MTT assay. Concentrations are based on Ag<sup>+</sup> ion concentrations in QD solutions as determined by ICP-OES. This concentration range corresponds to 4.6–115  $\mu\text{g QDs per mL}$ .



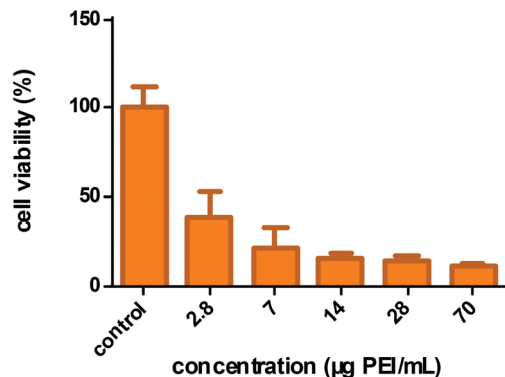


Fig. 7 Percent viability of HeLa cells exposed to PEI as determined by the MTT assay. These five PEI concentrations correspond to the maximum possible amount in Ag<sub>2</sub>S NIRQDs synthesized with 80/20 PEI/2MPA coatings and tested (Fig. 6). As an example, in 1.6 mg nanoparticles per mL there is 1 µg per mL Ag<sup>+</sup> and 2.8 µg per mL PEI.

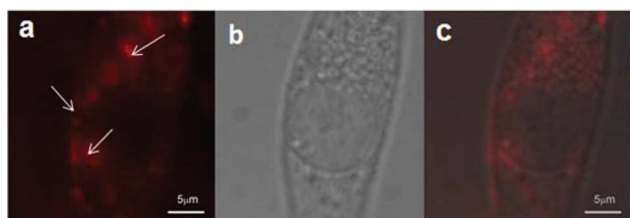


Fig. 8 Cellular uptake and localization of PEI/2MPA coated Ag<sub>2</sub>S NIRQDs by HeLa cells. Near-IR (a), transmission (b) merged images (c) of an individual cell. Red color shows the quantum dots. Arrows show some of the QDs in the cell.

ponent of the coating mixture with a tight binding to the crystal surface which is embedded in the relatively thicker PEI coating. Therefore, 2MPA did not interact with the cell, but PEI did. Therefore, at all doses, pure PEI or PEI/2MPA mixed coatings resulted in similar viability levels.

### Cell internalization and optical imaging

Strong emission in the NIR, cytocompatibility at low doses and effective gene delivery would make these particles excellent theranostic tools. For diagnostic purposes, strong intracellular signals originating from QDs are very important. Confocal images of the HeLa and MCF-7 cells incubated with Ag<sub>2</sub>S NIRQDs with 80/20 PEI/2MPA indicate an efficient cell internalization and endosomal localization of QDs with strong luminescence (Fig. 8), proving their potential as an optical probe. This optical signal originating from NIRQDs was dramatically stronger than the weak autofluorescence seen at this excitation wavelength (532 nm) (Fig. S11†).

### Use of Ag<sub>2</sub>S-PEI/2MPA NIRQDs in the *in vitro* transfection

To evaluate the potential of Ag<sub>2</sub>S NIRQDs coated with a PEI/2MPA mixture as gene delivery agents, a series of *in vitro* green fluorescence protein (pMax-GFP) transfection experiments

were performed with MCF-7 and HeLa cells. Commercial cell culture grade PEI (linear, 25 kDa) was used as a control. QDs were studied in a concentration range where no significant toxicity was detected ( $[Ag^+] = 1-2.5 \mu\text{g mL}^{-1}$ ,  $[QD] = 1-2.5 \mu\text{g mL}^{-1}$ ) (Fig. 6). As shown in Fig. 9, GFP transfection efficiency and expression levels were similar to or higher than commercial PEI (used at a standard, non-toxic dose) when the GFP vector was delivered using the Ag<sub>2</sub>S NIRQD above 1.5 µg per ml Ag<sup>+</sup> (6.9 µg per ml QD) concentration both in MCF-7 cells (Fig. 9) and in HeLa cells (Fig. 10).

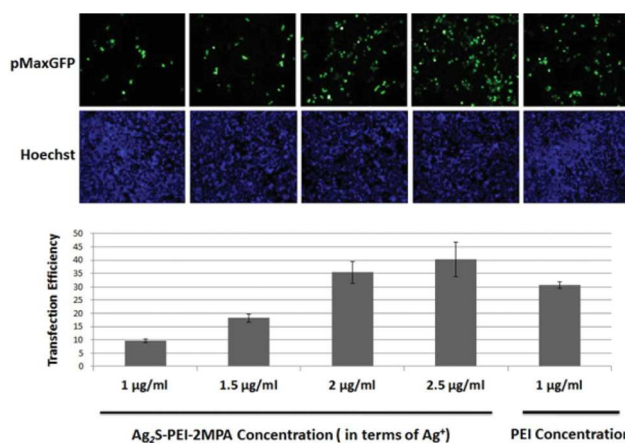


Fig. 9 Transfection of MCF-7 cells: (A) cells were transfected with the pMax-GFP plasmid using Ag<sub>2</sub>S-PEI/2MPA NIRQDs or control PEI (1 µg ml<sup>-1</sup>). Transfection efficiency was assessed using a fluorescence microscope. Hoechst staining was used to show the nuclei of all cells in the field. (B) Quantitative analysis of GFP positive cells in (A) (mean ± SD of independent experiments,  $n = 3$ ).

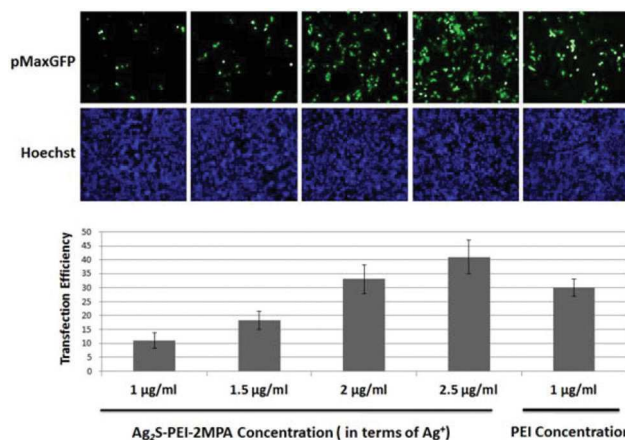
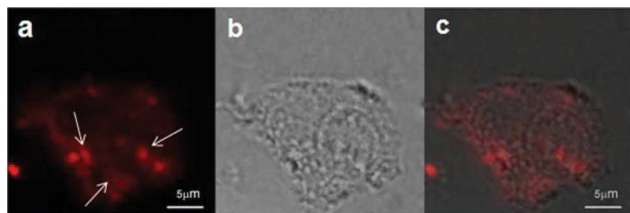


Fig. 10 Transfection of HeLa cells. (A) Cells were transfected with the pMax-GFP plasmid using Ag<sub>2</sub>S-PEI/2MPA NIRQDs or control PEI (1 µg ml<sup>-1</sup>). Transfection efficiency was assessed using a fluorescence microscope. Hoechst staining was used to show the nuclei of all cells in the field. (B) Quantitative analysis of GFP positive cells in (A) (mean ± SD of independent experiments,  $n = 3$ ).



**Fig. 11** Cellular uptake and localization of GFP loaded PEI/2MPA coated  $\text{Ag}_2\text{S}$  NIRQDs in MCF-7 cells. Near-IR (a), transmission (b) and merged images (c) of an individual cell. Arrows show QDs in the cell.

Highest transfection efficiencies achieved with  $\text{Ag}_2\text{S}$  NIRQDs were 41% for HeLa and 40% for MCF-7 cells. Under similar conditions, the transfection efficiency of commercial PEI was around 30% for both cell lines. Considering that the actual PEI content of the QD may be lower than anticipated, and free PEI at the corresponding doses would be too toxic to be used, this improvement over free PEI may be more significant than it seems.

The CLM images of the transfected MCF-7 cells with QDs (Fig. 11) demonstrate a strong optical signal originating from  $\text{Ag}_2\text{S}$ -PEI/2MPA NIRQDs proving the internalization of particles conjugated with pMax-GFP by the cells. These images prove the efficient uptake of QDs with and without the plasmid. These results confirmed that both DNA binding and intact DNA delivery capabilities of  $\text{Ag}_2\text{S}$ -PEI/2MPA QDs are better than those of commercial PEI 25 kDa, promoting these QDs as biocompatible theranostic nanoparticles.

## Conclusion

Theranostics has been very popular over the last decade, especially with the development of nanoparticles as drug carriers and imaging agents. The combined action of gene delivery and optical imaging is one of the most valuable capabilities in medicine and is moving towards near-infrared emitting quantum dots due to the many advantages described herein. The present study demonstrated a simple, aqueous preparation of cationic, cytocompatible  $\text{Ag}_2\text{S}$  quantum dots with the utilization of PEI and 2MPA mixed coatings and their potential as optical probes and gene delivery vehicles *in vitro*. The advantages of these NIRQDs are numerous: highest quantum yield reported so far (150%) may allow a reduction of the necessary dose for signal detection. Strong luminescence in the NIR-I window eliminates autofluorescence for a better signal-to-noise ratio and allows strong optical signals. Although PEI coatings provided poorly luminescent particles, the incorporation of 2MPA as a co-stabilizer provided a synergy and produced colloiddally stable particles with strong luminescence and smaller size crystals compared to PEI or 2MPA coated particles. Although a polymeric coating usually provides colloidal stability, it leaves defects on the crystal surface and causes poor luminescence due to the lack of dense packing

restricted by the polymer backbone. Hence, the addition of small strongly binding 2MPA both decreases the crystal size due to such strong Ag–thiol binding and passivates uncoordinated sites, increasing QY.

Significant advantages are gained in terms of cytotoxicity. Heavy metal related cytotoxicity was eliminated by using quite a biocompatible  $\text{Ag}_2\text{S}$  semiconductor core. PEI based toxicity was reduced by surface adsorption on the QD core, possibly due to the loss of some amines upon surface binding, and coexistence of 2MPA. Although not as cytocompatible as 2MPA coated  $\text{Ag}_2\text{S}$  NIRQDs, PEI/2MPA coated  $\text{Ag}_2\text{S}$  NIRQDs are cytocompatible below  $5 \mu\text{g Ag}^+$  per mL ( $23 \mu\text{g}$  per mL QD). Achieving cytocompatibility without PEGylation of the cationic particles is very important since PEGylation does interfere with the gene delivery potential and the endosomal escape of the nanoparticles. The absence of ligand exchange and PEGylation steps and direct coating of the QD core with the PEI/2MPA mixture also provided small sized particles, which is advantageous for prolonged blood circulation or for possible active targeting applications.

These NIRQDs were internalized by HeLa and MCF-7 cells and showed strong optical signals in CLM images. Additionally, these NIRQDs successfully transfected both of these cell lines with GFP. The transfection efficiency was about 40% following a standard protocol which shows 30% transfection efficiency with the control PEI (linear, 25 kDa). Possibly this can be optimized further and even better efficiencies can be obtained. With the rise of  $\text{Ag}_2\text{S}$  NIRQDs, we demonstrate the synthesis of highly luminescent, cationic QDs with the best known polymeric transfection agent, PEI, and point out the promise of  $\text{Ag}_2\text{S}$  as valuable new theranostic nanoparticles.

## Acknowledgements

The authors would like to thank Assoc. Prof. Ozgur Birer (Koc University, Istanbul, Turkey) for the construction of a home-made PL instrument, Dr Baris Yagci (KUYTAM, Koc University, Istanbul, Turkey) for XPS and Assoc. Prof. Mehmet Ali Gulgun (Sabanci University, Istanbul, Turkey) for TEM analysis.

## Notes and references

- 1 N. Nayerossadat, T. Maedeh and P. A. Ali, *Adv. Biomed. Res.*, 2012, **1**, 27.
- 2 T. G. Park, J. H. Jeong and S. W. Kim, *Adv. Drug Delivery Rev.*, 2006, **58**, 467–486.
- 3 C. W. Pouton and L. W. Seymour, *Adv. Drug Delivery Rev.*, 2001, **46**, 187–203.
- 4 J. M. Dang and K. W. Leong, *Adv. Drug Delivery Rev.*, 2006, **58**, 487–499.
- 5 G. A. Hussein and W. G. Pitt, *Adv. Drug Delivery Rev.*, 2008, **60**, 1137–1152.
- 6 I. Honoré, S. Grosse, N. Frison, F. Favatier, M. Monsigny and I. Fajac, *J. Controlled Release*, 2005, **107**, 537–546.

- 7 G.-J. Jeong, H.-M. Byun, J. M. Kim, H. Yoon, H.-G. Choi, W.-K. Kim, S.-J. Kim and Y.-K. Oh, *J. Controlled Release*, 2007, **118**, 118–125.
- 8 S. Patil, D. Rhodes and D. Burgess, *AAPS J.*, 2005, **7**, E61–E77.
- 9 Y. Lee, *Bull. Korean Chem. Soc.*, 2008, **29**, 666–668.
- 10 Y. Li, X. Duan, L. Jing, C. Yang, R. Qiao and M. Gao, *Biomaterials*, 2011, **32**, 1923–1931.
- 11 H. Duan and S. Nie, *J. Am. Chem. Soc.*, 2007, **129**, 3333–3338.
- 12 E. Q. Song, Z. L. Zhang, Q. Y. Luo, W. Lu, Y. B. Shi and D. W. Pang, *Journal*, 2009, **55**, 955–963.
- 13 A. Masotti, P. Vicennati, F. Boschi, L. Calderan, A. Sbarbati and G. Ortaggi, *Bioconjugate Chem.*, 2008, **19**, 983–987.
- 14 R. Aswathy, Y. Yoshida, T. Maekawa and D. S. Kumar, *Anal. Bioanal. Chem.*, 2010, **397**, 1417–1435.
- 15 S. B. Rizvi, S. Ghaderi, M. Keshtgar and A. M. Seifalian, *Nano Rev.*, 2010, **1**, DOI: 10.3402/mamo.v1i0.5161.
- 16 Y. Lu, Y. Su, Y. Zhou, J. Wang, F. Peng, Y. Zhong, Q. Huang, C. Fan and Y. He, *Biomaterials*, 2013, **34**, 4302–4308.
- 17 Y.-H. Chien, Y.-L. Chou, S.-W. Wang, S.-T. Hung, M.-C. Liao, Y.-J. Chao, C.-H. Su and C.-S. Yeh, *ACS Nano*, 2013, **7**, 8516–8528.
- 18 J. O. Escobedo, O. Rusin, S. Lim and R. M. Strongin, *Curr. Opin. Chem. Biol.*, 2010, **14**, 64–70.
- 19 B. L. Wehrenberg, C. Wang and P. Guyot-Sionnest, *J. Phys. Chem. B*, 2002, **106**, 10634–10640.
- 20 L. Bakueva, I. Gorelikov, S. Musikhin, X. S. Zhao, E. H. Sargent and E. Kumacheva, *Adv. Mater.*, 2004, **16**, 926–929.
- 21 M. T. Harrison, S. V. Kershaw, M. G. Burt, A. Eychmüller, H. Weller and A. L. Rogach, *Mater. Sci. Eng., B*, 2000, **69–70**, 355–360.
- 22 K. Schumann, *Z. Ernährungswiss*, 1990, **29**, 54–73.
- 23 P. Jiang, C. N. Zhu, Z. L. Zhang, Z. Q. Tian and D. W. Pang, *Biomaterials*, 2012, **33**, 5130–5135.
- 24 J. Chen, T. Zhang, L. Feng, M. Zhang, X. Zhang, H. Su and D. Cui, *Mater. Lett.*, 2013, **96**, 224–227.
- 25 P. Jiang, Z.-Q. Tian, C.-N. Zhu, Z.-L. Zhang and D.-W. Pang, *Chem. Mater.*, 2011, **24**, 3–5.
- 26 Y. Wang and X.-P. Yan, *Chem. Commun.*, 2013, **49**, 3324–3326.
- 27 Y. Zhang, Y. Zhang, G. Hong, W. He, K. Zhou, K. Yang, F. Li, G. Chen, Z. Liu, H. Dai and Q. Wang, *Biomaterials*, 2013, **34**, 3639–3646.
- 28 Y. Zhang, G. Hong, Y. Zhang, G. Chen, F. Li, H. Dai and Q. Wang, *ACS Nano*, 2012, **6**, 3695–3702.
- 29 G. Hong, J. T. Robinson, Y. Zhang, S. Diao, A. L. Antaris, Q. Wang and H. Dai, *Angew. Chem., Int. Ed.*, 2012, **51**, 9818–9821.
- 30 H. Y. Yang, Y. W. Zhao, Z. Y. Zhang, H. M. Xiong and S. N. Yu, *Nanotechnology*, 2013, **24**, 055706.
- 31 M. Yarema, S. Pichler, M. Sytnyk, R. Seyrkammer, R. T. Lechner, G. Fritz-Popovski, D. Jarzab, K. Szendrei, R. Resel, O. Korovyanko, M. A. Loi, O. Paris, G. Hesser and W. Heiss, *ACS Nano*, 2011, **5**, 3758–3765.
- 32 Y. Du, B. Xu, T. Fu, M. Cai, F. Li, Y. Zhang and Q. Wang, *J. Am. Chem. Soc.*, 2010, **132**, 1470–1471.
- 33 C. Li, Y. Zhang, M. Wang, Y. Zhang, G. Chen, L. Li, D. Wu and Q. Wang, *Biomaterials*, 2014, **35**, 393–400.
- 34 G. Chen, F. Tian, Y. Zhang, Y. Zhang, C. Li and Q. Wang, *Adv. Funct. Mater.*, 2014, **24**, 2481–2488.
- 35 I. Hocaoglu, M. N. Çizmeciyen, R. Erdem, C. Ozen, A. Kurt, A. Sennaroglu and H. Y. Acar, *J. Mater. Chem.*, 2012, **22**, 14674.
- 36 S. Celebi, A. K. Erdamar, A. Sennaroglu, A. Kurt and H. Y. Acar, *J. Phys. Chem. B*, 2007, **111**, 12668–12675.
- 37 H. Y. Acar, R. Kas, E. Yurtsever, C. Ozen and I. Lieberwirth, *J. Phys. Chem. C*, 2009, **113**, 10005–10012.
- 38 A. M. Smith, H. Duan, M. N. Rhyner, G. Ruan and S. Nie, *Phys. Chem. Chem. Phys.*, 2006, **8**, 3895–3903.
- 39 H. Li, W. H. Shih, W. Y. Shih, L. Chen, S. J. Tseng and S. C. Tang, *Nanotechnology*, 2008, **19**, 475101.
- 40 A. M. Mohs, H. Duan, B. A. Kairdolf, A. M. Smith and S. Nie, *Nano Res.*, 2009, **2**, 500–508.
- 41 Y. Zhang, J. M. Liu and X. P. Yan, *Anal. Chem.*, 2013, **85**, 228–234.
- 42 G. H. Au, W. Y. Shih, S. J. Tseng and W. H. Shih, *Nanotechnology*, 2012, **23**, 275601.
- 43 A. Zintchenko, A. S. Sussha, M. Concia, J. Feldmann, E. Wagner, A. L. Rogach and M. Ogris, *Mol. Ther.*, 2009, **17**, 1849–1856.
- 44 A guide to recording fluorescence quantum yields <http://www.horiba.com/fileadmin/uploads/Scientific/Documents/Fluorescence/quantumyieldstrad.pdf>.
- 45 H. Li, W. Y. Shih and W.-H. Shih, *Ind. Eng. Chem. Res.*, 2007, **46**, 2013–2019.
- 46 S. Choosakoonkriang, B. A. Lobo, G. S. Koe, J. G. Koe and C. R. Middaugh, *J. Pharm. Sci.*, 2003, **92**, 1710–1722.
- 47 J. D. Ziebarth and Y. Wang, *Biomacromolecules*, 2010, **11**, 29–38.
- 48 A. von Harpe, H. Petersen, Y. Li and T. Kissel, *J. Controlled Release*, 2000, **69**, 309–322.
- 49 H. Y. Acar, S. Celebi, N. I. Serttunali and I. Lieberwirth, *J. Nanosci. Nanotechnol.*, 2009, **9**, 2820–2829.
- 50 O. Madelung, *Semiconductors: Data Handbook*, Springer Verlag, Berlin, Heidelberg, Newyork, 2004.
- 51 R. Chen, N. T. Nuhfer, L. Moussa, H. R. Morris and P. M. Whitmore, *Nanotechnology*, 2008, **19**, 455604.
- 52 J. Li, W. Tang, H. Yang, Z. Dong, J. Huang, S. Li, J. Wang, J. Jin and J. Ma, *RSC Adv.*, 2014, **4**, 1988.